Research Article | Vol. 26, No. 11 | 28 May 2018 | OPTICS EXPRESS 14038
Optics EXPRESS

Metameric MIMO-OOK transmission scheme using multiple RGB LEDs

THAI-CHIEN BUI, ROBERTO CUSANI, GAETANO SCARANO, AND MAURO BIAGI*

Department of Information, Electrical and Telecommunication (DIET) Engineering, "Sapienza" University of Rome, Via Eudossiana 18, 00184 *Rome, Italy*
Mauro.Biagi@uniroma1.it

Abstract: In this work, we propose a novel visible light communication (VLC) scheme utilizing multiple different red green and blue triplets each with a different emission spectrum of red, green and blue for mitigating the effect of interference due to different colors using spatial multiplexing. On-off keying modulation is considered and its effect on light emission in terms of flickering, dimming and color rendering is discussed so as to demonstrate how metameric properties have been considered. At the receiver, multiple photodiodes with color filter-tuned on each transmit light emitting diode (LED) are employed. Three different detection mechanisms of color zero forcing, minimum mean square error estimation and minimum mean square error equalization are then proposed. The system performance of the proposed scheme is evaluated both with computer simulations and tests with an Arduino board implementation.

© 2018 Optical Society of America under the terms of the OSA Open Access Publishing Agreement

OCIS codes: (060.2605) Free-space optical communication; (060.4080) Modulation.

References and links

1. M. Biagi, A. M. Vegni, S. Pergoloni, P. M. Butala, and T. D. C. Little, "Trace-orthogonal PPM-space time block coding under rate constraints for visible light communication," J. Lightw. Technol. **33**(2), 481–494 (2015).
2. Y. Chen and M. Jiang, "Joint colour-and-spatial modulation aided visible light communication system," in *Proceedings of IEEE 83rd Vehicular Technology Conference* (IEEE, 2016), pp. 1–5.
3. P. M. Butala, H. Elgala, and T. D. C. Little, "SVD-VLC: a novel capacity maximizing VLC MIMO system architecture under illumination constraints," in *Proceedings of IEEE Globecom Workshops* (IEEE, 2013), pp. 1087–1092.
4. J. Armstrong, Y. Sekercioglu, and A. Neild, "Visible light positioning: a roadmap for international standardization," IEEE Commun. Mag. **51**(12), 68–73 (2013).
5. T.-H. Do, J. Hwang, and M. Yoo, "TDoA based indoor visible light positioning systems," in *Proceedings of International Conference on Ubiquitous and Future Networks* (IEEE, 2013), pp. 458–458.
6. M. Biagi, S. Pergoloni, and A. M. Vegni, "LAST: a framework to localize, access, schedule, and transmit in indoor VLC systems," J. Lightw. Technol. **33**(9), 1872–1887 (2015).
7. N. Fujimoto and S. Yamamoto, "The fastest visible light transmissions of 662 Mb/s by a blue LED, 600 Mb/s by a red LED, and 520 Mb/s by a green LED based on simple OOK-NRZ modulation of a commercially available RGB-type white LED using pre-emphasis and post-equalizing techniques," in *Proceedings of the European Conference on Optical Communication* (IEEE, 2014), pp. 1–3.
8. K. D. Langer, J. Vucic, C. Kottke, L. FernÃ¡ndez, K. Habe, A. Paraskevopoulos, M. Wendl, and V. Markov, "Exploring the potentials of optical-wireless communication using white leds," in *Proceedings of the International Conference on Transparent Optical Networks* (IEEE, 2011), pp. 1–5.
9. H. Chun, S. Rajbhandari, G. Faulkner, D. Tsonev, E. Xie, J. J. D. McKendry, E. Gu, M. D. Dawson, D. C. O'Brien, and H. Haas, "LED based wavelength division multiplexed 10 Gb/s visible light communications," J. Lightw. Technol. **34**(13), 3047–3052 (2016).
10. R. Jiang, Z. Wang, Q. Wang, and L. Dai, "Multi-user sum-rate optimization for visible light communications with lighting constraints," J. Lightw. Technol. **34**(16), 3943–3952 (2016).
11. Q. Gao, C. Gong, and Z. Xu, "Joint transceiver and offset design for visible light communications with input-dependent shot noise," IEEE Trans. on Wireless Commun. **16**(5), 2736 –2747 (2017).
12. A. K Jain, "*Fundamentals of digital image processing*," (Prentice-Hall, Inc., 1989), Chap. 3.
13. S. Pergoloni, M. Biagi, S. Colonnese, R. Cusani, and G. Scarano, "Coverage optimization of 5G atto-cells for visible light communications access," in *Proceedings of the IEEE International Workshop on Measurements Networking* (IEEE, 2015), pp. 1–5.
14. J. M. Kahn, and J. R. Barry, "Wireless infrared communications," Proceedings of the IEEE **85**(2), 265–298 (1997).

#319327 https://doi.org/10.1364/OE.26.014038
Journal © 2018 Received 9 Jan 2018; accepted 3 Apr 2018; published 17 May 2018

Optics EXPRESS

15. M. Uysal, F. Miramirkhani, O. Narmanlioglu, T. Baykas, and E. Panayirci, "IEEE 802.15.7r1 reference channel models for visible light communications," in IEEE Commun. Mag. **55**(1), 212 –217 (2017)
16. F. Miramirkhani, O. Narmanlioglu, M. Uysal, and E. Panayirci, "A mobile channel model for VLC and application to adaptive system design," in IEEE Commun. Lett. **21**(5), 1035 –1038 (2017).
17. S. R. Perez, R. P. Jimenez, O. B. G. Hernandez, R. Borges, and R. Mendoza, "Concentrator and lens models for calculating the impulse response on IR-wireless indoor channels using a ray-tracing algorithm," Microw. Opt. Technol. Lett. **36**(4), 262–267 (2003).
18. M. Rupp, "Robust design of adaptive equalizers," IEEE Trans. Signal Process. **60**(4), 1612–1626 (2012).
19. M. Rahaim, T. Borogovac, and J. B. Carruthers, "CandLES: communications and lighting emulation software," in *Proceedings of the fifth ACM international workshop on Wireless network testbeds, experimental evaluation and characterization* (ACM, 2010), pp. 9–14.
20. A. Burton, H. Le Minh, Z. Ghassemlooy, E. Bentley, and C. Botella, "Experimental demonstration of 50-Mb/s visible vight communications using 4 x 4 MIMO," Photon. Technol. Let. **26**(9), 945–948 (2014).
21. Luxeon Star LEDs, *Rebel LEDs datasheet* (Luxeon Star LEDs, 2016).
22. Vishay, *Vishay BPW34 data sheet* (Vishay, 2016).
23. G. Wyszecki and W. S. Stiles, *Color Science* (Wiley Classic Library, 2000).

1. Introduction and goals

Due to the proliferation of personal mobile devices connected to the Internet, the need of exchanging a large amount of data at very high speed has considerably increased during the last years, and this trend will continue in the future. Addressing this issue, visible light communication (VLC) can be a very effective complementary technology to existing radio frequency (RF). VLC systems do not suffer from RF interference and they can be adopted in places like airplanes and hospitals where the use of RF technology is partially or totally limited. Besides, light emitting diodes (LEDs) are more power efficient devices than incandescent lamps, and they also provide data transmission while illuminating. Stating this twofold application, VLC system meets the requirements for reducing the global electromagnetic pollution and is currently a viable and promising technology both for providing data communications [1–3] and localization [4–6].

Due to its simple implementation, on-off keying (OOK) is the simplest used intensity modulation/direct detection (IM/DD) scheme with VLC technology. It is possible to achieve very high data rates even adopting OOK not-return to zero (NRZ) modulation, as demonstrated by Fujimoto et al. [7], where a system including a single commercially available red, green and blue (RGB) visible LED, a low-cost PIN-PD and pre-emphasis and post-equalizing blocks is presented. High-speed VLC systems employing different modulation schemes, such as OOK, applied to RGB LED light sources are investigated experimentally at Heinrich Hertz Institute [8]. Depending on modulation format, link distance and receiver sensitivity, communication data rates up to 800 Mb/s have been demonstrated using off-the-shelf optical components. More, as white LED consists of red, green and blue chips (i.e. RGB LEDs), the employment of wavelength division multiplexing (WDM) is introduced to increase the data transmission rate. The chance of simultaneously sending an independent data stream on different color components according to WDM is tackled in a recent research [9]. Specifically, it is shown that a rate adaptive scheme used in a LED-based communication can lead to an aggregate data rate beyond 10 Gb/s. Also in this case channel knowledge at the transmitter is required. Moreover, the cross-talk interference, that is the interference generated by different colors, at the receiver is neglected by the use of dichroic mirrors. This is a viable solution even though it fails to work if multiple red, blue or green light are used, that is, when an array of LEDs is adopted. In fact, using multiple LEDs increases the spectral efficiency of the system. Recently, some works have been done in consideration of multiuser scheme for VLC system employing RGB-LEDs at the transmitter. A multiuser multiple-input-single-output (MISO)-VLC system that employs multi-chip LEDs with different colors at the transmitter is proposed [10]. At the receiver, each user is equipped with a PD that utilizes an optical filter to concentrate on a corresponding monochromatic light of a specific LED chip. That work aims also at maximizing the multiuser sum rate by proposing an electrical and

Optics EXPRESS

optical power allocation scheme with constraints on illumination. A joint transceiver and offset design method are proposed and analyzed for both the single user point-to-point and the multiuser MISO uplink and downlink systems in [11] where the transmitter consists of two triplets of RGB-LEDs and the receiver equipped with six photodiode (PD) detectors, each with red, green and blue filters. Input-dependent shot noise is taken into consideration when evaluating the performance of such system. That system aims at using precoding by assuming perfect channel knowledge at the transmitter and receiver by assuming also some specific channel configurations without taking into account LED and photodiode characteristics, nor implementation. However, the iterative algorithm requires complexity of the order to seconds to work that is not of practical implementation.

After the literature review, it appears that multiple-input-multiple-output (MIMO) schemes including the use of multiple colors (more than the simple single red, green and blue configuration) as a viable road for improving spectral efficiency with the goal of obtaining white light as illumination service has not been tackled both from theoretical and experimental point of view. In this context, we propose and demonstrate the possibility of using multiple RGB-LEDs (multiple triplets) for spatial multiplexing. Specifically, each RGB-LED is assumed to have slightly different emission spectra so that the red LED of the first RGB-LED is different (from the spectral point of view) from the red LED of other RGB-LED and similarly for green and blue LEDs. Doing this allows us to multiplex independent information on each LED and the effect of color interference, that is color cross-talk, is investigated.

Furthermore, we design the proposed system with constraint on illumination by taking into account color-rendering, flickering and discussing about dimming. Besides, three different type of detection mechanisms are then applied and analyzed. Those are color zero forcing (CZF), minimum mean square error (MMSE) without channel estimation and minimum mean square error (MMSE) with channel equalization. The scheme presents the transmission of pilot symbols that can be used for channel estimation due to its possible variability caused by the receiver mobility in a room. The performance is evaluated both with computer simulations and tests with an Arduino board implementation.

About paper organization, in Sect.2 we detail the system model while in Sect.3 we present both zero forcing and minimum mean square error equalization methods applied to the proposed scheme. Furthermore, we present the performance of the proposed architecture in Sect.4 and we compare it with the literature in Sect.4.1. The implementation on a Arduino board is described and tests reported in Sect.5 while in Sect.6 we draw conclusion.

2. System model

Let us consider the presence of N_t LED triplets, so having $3N_t$ LEDs at the transmitter. Each triplet is characterized by red green and blue colors and the red of the first triplet is different, from a spectral point of view, from the red of the second triplet and so forth, and the same is also for green and blue. In Fig. 1 we show the system architecture including the presence of multiple LEDs. The transmitted signal during the signaling interval T_p by the i-th LED triplet is given by:

$$x_i(t) = \sum_{c_i \in C_i} \gamma_{c_i} s_{c_i}(t) \tag{1}$$

where c_i belongs to the set $C_i = \{R_i, G_i, B_i\}, i = 1, ..., N_t$ that collects the three colors emitted by the i-th triplet. The term γ_{c_i} is a binary value and represents the OOK symbol emitted by the c color of the i-th triplet. Moreover, $s_{c_i}(t)$ is the shape of radiation representing the light emitted by the c_i-th color LED of the i-th triplet. It is important to note that when we consider two different

Optics EXPRESS

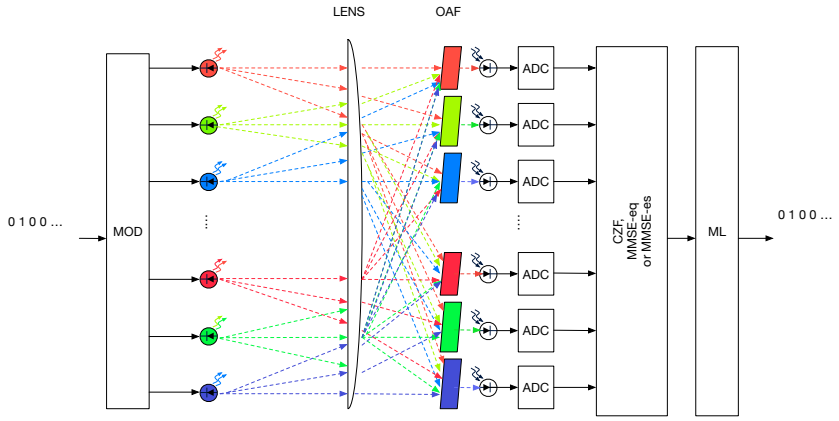

Fig. 1. Scheme of the transmitter, channel and receiver.

colors, namely c_i and c_l, we have $s_{c_i}(t) \neq s_{c_l}(t)$. Hence, the whole transmitted signal is given by

$$x(t) = \sum_{i=1}^{N_t} x_i(t) = \sum_{i=1}^{N_t} \sum_{c_i \in C_i} \gamma_{c_i} s_{c_i}(t). \tag{2}$$

In order to avoid ambiguity, we name the emission in the signalling time of a single pulse (or its absence) as OOK symbol, while we indicate the triplet of OOK symbols emitted during T_p with RGB-OOK symbol and we call the $3N_t$-ple of OOK symbols emitted by all the available LEDs in the signaling interval T_p as MIMO-RGB-OOK symbol.

Regarding Eq. (1), the presence of the term γ_{c_i} implicitly leads the transmitter to emit different light intensities over the time since each LED (R, G and B) can be in the on or off state. Hence, before proceeding, we go in depth with some possible issues related to light and color perception. Even though we turn on and off the light, Bloch's law [12, Chapt.3] ensures that flickering effects are avoided if OOK symbol transmission rate is kept above 50-100 Hz.

About dimming, we can recognize that the proposed system has a limited support. In fact, while OOK itself presents a 50% dimming with respect to full illumination, we can define dimming as the full illumination (no modulation) when we use $3N_t$ LEDs. If we choose, due to possible system requirements, to use a lower number of LEDs with the respect to the maximum allowed (let us say $3M_t$), we achieve a dimming level given by $(M_t/N_t)\cdot 50\%$.

Furthermore, since the light radiation is able to excite the retina [12][Chapt.2], the second Bloch's law still allows us to state that the eye is unable to follow the on-off transitions. In fact, when the light beam impacts on the retina, the sensation is hold for approximately 20ms that is the integration time of the visual system and after the light will impress a new image (this is also the effect on the basis of television). About color rendering some insight should be given.

Optics EXPRESS

By resorting to the CIE 1931 diagram reported in Fig. 2, we show how choosing one triplet of primary colors can allow the representation of each color in the area defined by the triangle whose vertexes are identified by the primaries. and the lines connecting the vertexes represent the

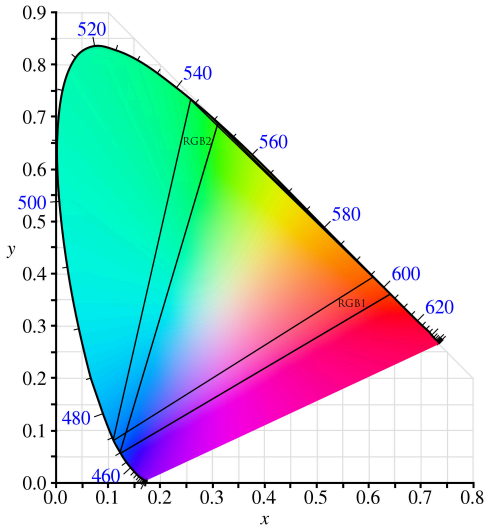

Fig. 2. CIE 1931 diagram with primaries and regions of affordable colors with two triplets of primaries.

bounds of the region collecting all the colors that can be obtained. Hence, we show in Fig. 2 the colors that can be represented with a first triplet (RGB1) and with a second triplet (RGB2). Both the triplets are able to obtain white light. However, since the light emitted is tied to the MIMO-RGB-OOK symbol that the transmitter is emitting, it is possible that, for example, red and blue are on while green is off (so generating a magenta hue). Moreover, we must note that the whole human vision system works on the basis of the above mentioned integration time, that is, 20ms. This implies that the sensation is the time average measured on that interval. This implicitly corresponds to say that the eye *sees* the short time Fourier transform that, in this case, is characterized by essentially N_t different whites whose combination still falls in the white area of the CIE 1931 diagram. This consideration is based on the principle of metamerism [12][Chapt.2] and justifies the choice of the wavelength of the signals emitted by the triplets.

Moving on the signal that is received by the j-th photodiode, with $c_j \in C_i$, related to the emission of a single MIMO-RGB-OOK symbol we have that

$$y_{c_j}(t) = \sum_{i=1}^{N_t} \sum_{c_i \in C_i} \gamma_{c_i} s_{c_i}(t) * h_{c_i,c_j}(t) + w_{c_j}(t) \tag{3}$$

where $*$ is the convolution operator, $h_{c_i,c_j}(t)$ is the whole channel impulse response from LED emitting the c_i color to the photodiode tuned on the c_j one, while $w_{c_j}(t)$ describes the noise. Before proceeding it is mandatory to explain the role played by $h_{c_i,c_j}(t)$ and the different features that compose the channel impulse response. The term $h_{c_i,c_j}(t)$ can be exploded as follows

$$h_{c_i,c_j}(t) = f_{FSP_{c_i,c_j}}(t) * f_L(t) * f_{cj}(t) * f_{PD}(t) \tag{4}$$

where $f_{FSP_{c_i,c_j}}(t)$ is the effect of free space propagation that can be modeled according to geometrical parameters. More insight about this can be found in [13] where the propagation

Optics EXPRESS

features of the channel have been detailed. Summarizing, we can affirm that we resort to Lambertian model (see [14]) and the propagation environment is non-directed line-of-sight (LOS) thus meaning that we are in the presence of a main component (LOS) and some reflective paths. Recently additional insights have been considered in the Literature by showing how delay spread is around tens of nanoseconds [15,16]. Moreover, $f_L(t)$ in Eq. (4) models the effect of the lens (if present) used to focus the light beam as depicted in Fig. 1 and its modeling can follow the work presented in [17]. Furthermore, $f_{cj}(t)$ in Eq. (4) is the impulse response of the OAF represented by the above mentioned colored transparent stripes whose modeling is relatively simple if, with a spectrum analyzer, a white light is used in order to test the wavelength response. Last, $f_{PD}(t)$ in Eq. (4) is the impulse response of the photodiode. It is worth providing an example about the role played by OAF. In fact, while it is reasonable to expect that the OAF of a red tuned photodiode is able to reduce the effect of blue light, it is not the same for the red emitted by another triplet. Let us say that the best approach that one can pursue is having the light spectrum of same color emitted by different triplets separated in the wavelength domain. As it will result clearer in the following this is not so simple with LEDs while in principle it can be affordable with lasers.

3. Detection mechanisms

We need to preliminary sample the received signal y_{c_j} after each photodiode so to have $y_j(nT_s)$, T_s being the sample time. This operation is performed by the analog to digital converter (ADC) as depicted in Fig.1. In this way, by extending this mechanism to all the RGB components we obtain, by assuming $T_s = T_p$, the following analytical description:

$$\mathbf{Y} = \mathbf{SH} + \mathbf{W} \tag{5}$$

where $\mathbf{S}$ is a $(M \times 3N_t)$ matrix collecting the M MIMO-RGB-OOK symbols emitted by the $3N_t$ LEDs during the coherence time T_{coh} of the channel with $M = \lfloor T_{coh}/T_p \rfloor$ while $\mathbf{W}$ gathers the $(M \times 3N_t)$ noise samples. Since we deal with OOK symbols the generic element of $\mathbf{S}$ is a zero or the light intensity associated to the *on* signal. We remark that the OOK stream on one LED is independent from the other ones. We additionally define as $\mathcal{S}$, the set collecting all the possible combinations $(2^{3N_t M})$ of matrices $\mathbf{S}$. Furthermore, $\mathbf{H}$ collects the $3N_t \times 3N_t$ channel impulse responses as given in Eq. (4) in which each component is assumed to be sufficiently short in time to be modeled as a coefficient. Before proceeding, some analysis on the assumption made on $\mathbf{H}$ are mandatory. By observing the modeling provided in the previous section for what concerns transmitter and channel, we can argue that if the transmission speed is not so high with respect to photodiode bandwidth, this latter is able to *follow* the speed of LED. Otherwise we need time (or frequency)-based equalization. Here we focus on the first case even though we discuss about this issue in the numerical results.

We compare here two different detection mechanisms, namely, spatial Zero-Forcing, that in this case means Color Zero Forcing (CZF) and Minimum Mean Square Error (MMSE) by implementing this latter in two different ways.

3.1. Color zero forcing

The CZF method aims at inverting the channel by using the inverse matrix of $\mathbf{H}$, that is, a spatial filter $\mathbf{Z} = \mathbf{H}^{-1}$ so as to obtain

$$\mathbf{X} = \mathbf{YZ} = \mathbf{S} + \mathbf{WH}^{-1}. \tag{6}$$

Two important elements must be underlined. First, in order to proceed with this approach, knowledge about the channel is required at the receiver. This can be inferred by transmitting periodically a training sequence characterized by $\mathbf{S} = \mathbf{I}_{3N_t}$ so as to have

$$\mathbf{Y}_{training} = \mathbf{H} + \mathbf{W} \tag{7}$$

and we consider the estimated channel $\tilde{\mathbf{H}} = \mathbf{Y}_{training}$. Hence the matrix inversion will be operated on the basis of the estimated one so Eq. (6) should be rewritten as follows

$$\mathbf{X} = \mathbf{S}\mathbf{H}\tilde{\mathbf{H}}^{-1} + \mathbf{W}\tilde{\mathbf{H}}^{-1}. \tag{8}$$

Second, another issue to be tackled is about the inversion of the channel matrix. Spatially speaking it is possible, especially in line of sight propagation, that some paths present spatial correlation, that is, the channel matrix has not full rank. We can observe that in order to avoid this situation we can space LEDs and photodiodes. Moreover, since the channel matrix considers also the effect of OAF the channel $\mathbf{H}$ can be interpreted as the Hadamard product of two matrices representing different terms of the whole channel, where the first one, $\mathbf{H}_1$ takes into account the propagation $f_{FSP_{c_i,c_j}}(t)$, photodiode $f_{PD}(t)$ and lens $f_L(t)$ effects, while the second one $\mathbf{H}_2$ only models the OAF behavior. Hence, we can write $\mathbf{H} = \mathbf{H}_1 \circ \mathbf{H}_2$.

About the decision mechanism, this latter can be described by the following expression that comes from the application of the maximum likelihood criterion by assuming that noise presents white Gaussian statistics:

$$\hat{\mathbf{S}} = \underset{\mathbf{S}\in\mathcal{S}}{\operatorname{argmin}} ||\mathbf{X} - \mathbf{S}||^2. \tag{9}$$

At a first glance, Eq. (9) appears to be costly to be solved since finding the above minimum should imply to check among $2^{3N_t M}$ matrices. Just to give a quick example, if $N_t = 4$ and $M = 10$, the number of comparisons to perform is 2^{120} that is not viable in real systems. However, we must highlight that we deal with OOK and the symbol detection requires a threshold mechanism. This implies that we can detect the $3N_t$ signals present in the $3N_t$ photodiode branches as shown in Fig.1 in parallel, every T_p seconds.

3.2. Minimum mean square error

In this section differently from the above cited CZF mechanism we will discuss about the possible implementation of MMSE criterion. We follow two different approaches to arrive at the detection phase. The first one does not require to directly estimate the channel and it aims at estimating $\mathbf{S}$ while the second one requires channel estimation in order to perform equalization. To handle this, we resort to the Orthogonal Projection Lemma (OPL) due to the Gaussianity of the problem. Hence, we have that the observation should be orthogonal to the error when deriving the MMSE filter. This means that we have

$$\tilde{\mathbf{S}} = \mathbf{Y}\mathbf{G} \tag{10}$$

and we can derive $\mathbf{G}$ as follows by using the OPL

$$E\left\{[\mathbf{S} - \mathbf{Y}\mathbf{G}]^T \ \mathbf{Y}\right\} = \mathbf{0} \tag{11}$$

$E(.)$ the expected value operator, and with very simple algebra we can write

$$\mathbf{G} = \left[\mathbf{R}_{YS}\mathbf{R}_{YY}^{-1}\right]^T \tag{12}$$

where $\mathbf{R}_{YY}$ is the autocorrelation related to the received matrix and $\mathbf{R}_{YS}$ is the crosscorrelation between the input (transmitted) and output (received). As for CZF case, while $\mathbf{R}_{YY}$ is based on what has been received, $\mathbf{R}_{YS}$ should require to know what has been transmitted. However, handling $\mathbf{R}_{YS}$ means to acquire, during a training phase, information about the above correlation. This implies that the estimated version of $\mathbf{R}_{YS}$ can be obtained via the following mechanism

$$\mathbf{R}_{YS} = \frac{1}{K}\sum_{k=1}^{K} \mathbf{Y}_k^T \mathbf{S}_k \tag{13}$$

Optics EXPRESS

where the term $\mathbf{S}_k$ represents the k-th matrix emitted as training that should be known by the receiver and $\mathbf{Y}_k$ is the k-th matrix received. We name this approach as MMSE estimation (MMSE-es) since we proceed to estimate $\mathbf{S}$. The other MMSE approach is the spatial equalization of the received matrix. This approach requires to estimate the channel $\mathbf{H}$ with a training sequence known at the receiver also including what has been described for CZF. Basing on the this latter and, more, by considering that $\mathcal{N}_0$ representing the noise power that can be estimated through a sufficiently long observation when the communication is not active, we can obtain the following expression by resorting to the equalization theory [18]

$$\mathbf{G} = \tilde{\mathbf{H}} \left(\tilde{\mathbf{H}}^T \tilde{\mathbf{H}} + \mathcal{N}_0 \mathbf{I} \right)^{-1}. \tag{14}$$

We name this approach as MMSE equalization (MMSE-eq). Also in the two MMSE mechanisms we can apply the maximum likelihood criterion so as to arrive at the following minimization

$$\hat{\mathbf{S}} = \underset{\mathbf{S} \in \mathcal{S}}{\operatorname{argmin}} ||\tilde{\mathbf{S}} - \mathbf{S}||^2. \tag{15}$$

The discussion after Eq. (8) is still valid here since the number of matrices comparison is huge. However, we newly highlight that basing on the fact that we have independent symbols we can perform detection according to threshold detectors and in particular, $3N_t$ parallel detectors detecting the symbol every T_p seconds, that is, at each row of $\tilde{\mathbf{S}}$.

4. Numerical results and implementation

We first evaluate the performance of the proposed system by performing computer simulations. These are performed by resorting to the channel model provided in [19] which takes into account the propagation in terms of reflections and direct path loss. Moreover, we use the parameters in line with the contribution in [20] with the exception of LEDs that in our contribution are RGB and not white. For what concerns LEDs, we refer to the Luxeon Star Rebel Red, Green and Blue whose features can be found in [21]. We use those LEDs for the implementation and summarize their key features in Table 1.

Table 1. Model Parameters

LED Transmitters	
Maximum transmit power	500mW
Beam angle	125° FWHM (Full Width Half Maximum)
Focus lens angle	60°
Transmitter pitch	2.5 cm
Receiver Vishay BPW34	
FOV	65°
wavelength range	430 nm - 1000 nm
maximum sensitivity wavelength	850 nm
Area	0.78 mm^2
Lens gain factor	2.2
Effective area A_e	3.3 mm^2
Receiver pitch	2.5 cm

Regarding receiver, we consider commercial photodiodes, namely Vishay BPW34. Also in this case the key parameters can be found in Table 1 while specifications are reported in [22]. The value for T_s is chosen so as to have 12.5 Mpulses/s on each branch. This choice is justified in

Optics EXPRESS

order to have a fair performance comparison with the scheme in [20], that is, the same symbol rate emitted by each LED. In all the performed tests/experiments we considered transmitter and receiver perfectly aligned thus meaning that the first LED faces the first photodiode and so forth.

4.1. Computer simulations

We show in Fig. 3 the BER obtained when $N_t = 2$ and consequently the rate is 75Mb/s when the receiver is located at a distance ranging from 140cm to 300cm. We report the BER for CZF, MMSE-es and MMSE-eq. It is possible to appreciate that the lowest BER values are obtained by MMSE-eq method while the MMSE-es is a bit worse. In fact, MMSE-es achieves BER values that is approximately twice the value of MMSE-eq. On the other hand CZF is a bit far from the

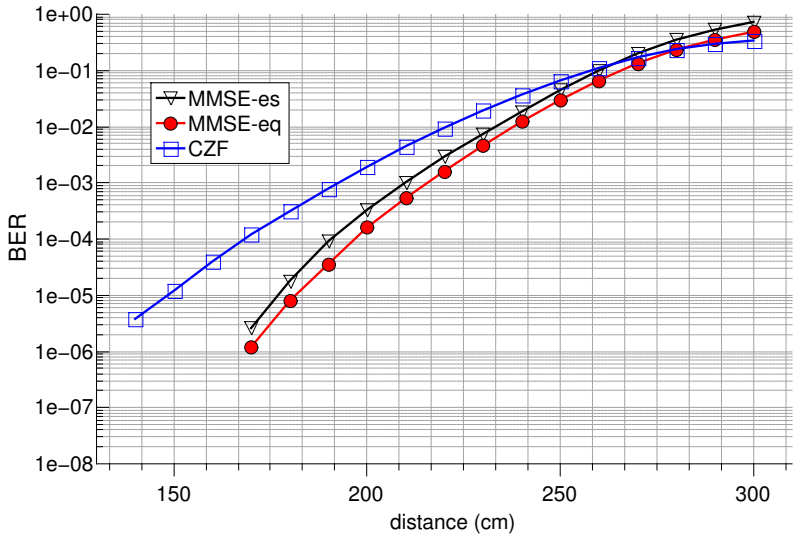

Fig. 3. BER as a function of distance between transmitter and receiver for the three detection methods when $N_t = 2$.

above two schemes especially for low distance where its performance is a BER of the order of $10^{-5} \div 10^{-6}$. When the distance increases the gap becomes less evident and at high distances CZF results to perform better than the other two even though the values are not acceptable for a communication system.

In Fig. 4 we compare the three detection methods with the contribution in [20] by assuming 70cm distance between transmitter and receiver. Moreover, we assume imperfect channel estimation at the receiver, that is, using a single pulse per LED. We recall that in [20] a 4x4 system is proposed and white LEDs are used. So, a perfect comparison is not possible since we adopt RGB LEDs. However, in this case, we can consider as comparison the cases characterized by $N_t = 1$ and $N_t = 2$. Before proceeding, it is important to specify that the rate values on the horizontal axis are simply obtained for different values of N_t.

It is possible to appreciate that the MMSE-eq is the best performing in terms of BER and for $N_t = 1$ its BER is below the system in [20]. Moreover, the BER achieved with $N_t = 2$ is still lower even though the transmission achieves 75Mb/s in place of 50Mb/s. By increasing the number of RGB triplets N_t we have that BER increases. The reason is the inability of the system in separating different components of same colors, for example red of the second triplet on the first red-tuned photodiode. This is due to the crosstalk among colors with very close (overlapping) spectra. In fact, if we neglect its presence, the system is still able to cancel interference

Optics EXPRESS

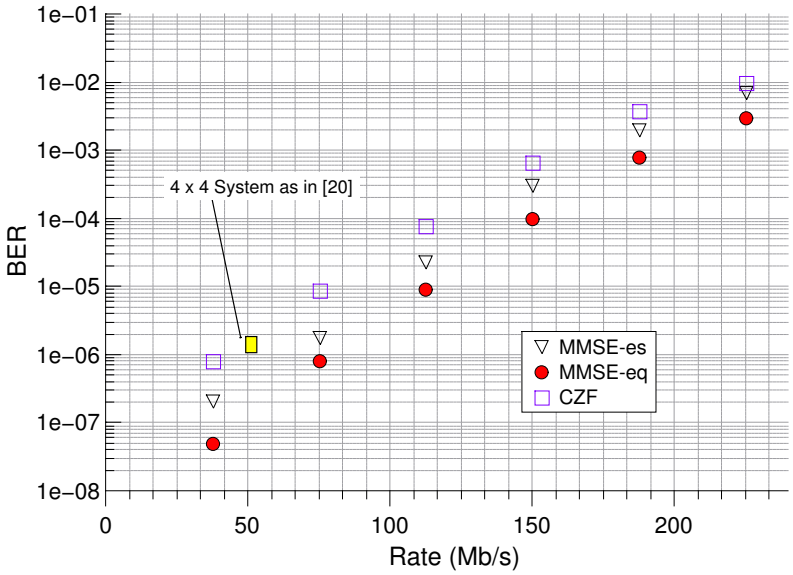

Fig. 4. BER as a function of transmission rate. Each marker corresponds to an increment of 3 RGB LEDs (that is N_t). Comparison with [20] is also reported.

Another way of increasing rate is to reduce signaling time T_p without increasing N_t. This implies that the symbols are much closer in time and possible intersymbol interference (ISI) can occur. In this regard, in Fig. 5 we report for the three detection mechanisms the BER achieved when the rate increases. Differently from Fig. 4 where the signaling time is assigned for each LED and we increase the number of triplets to increase rate, in Fig. 5 we consider $N_t = 1$ and reduce T_p on each LED from 75ns (40 Mb/s) to 12.5ns (240 Mb/s).

It is possible to appreciate that for low transmission rates the BER values achieved by the three detection methods approach those reported in Fig. 4 for rate equating 37.5 Mb/s. However, when we consider higher transmission rates the delay spread of the channels starts to increase BER since it induces intersymbol interference. Moreover, we can observe that the BER achieved are higher with respect to the case of Fig. 4. This can be justified by observing that the channels delay spread induces performance loss that is higher with respect to the one exhibited in Fig. 4 where the loss is due to the residual unsuppressed color interference. Moreover, increasing transmission rate till to very high values leads to additional ISI due to component limitations like LEDs and PDs. This suggests that, without using an equalizer that should be able also to track channel changes, using multiple RGB elements is preferable to increase rate. In Fig. 6 we report BER values as a function of distance between transmitter and receiver when MMSE-eq is used for detection. We report the BER curves for different number of triplets ranging from 1 to 4, thus meaning that, under the constraint of 12.5 Mpulses on each branch (LED) the total rate is 37.5 Mb/s for $N_t = 1$, 75 Mb/s for $N_t = 2$, 112.5 Mb/s for $N_t = 3$ and 150 Mb/s for $N_t = 4$.

In this case it is possible to appreciate that when the number of triplets is only one, the BER is the smallest. This can be justified by observing that no interference among the same color of different triplets occurs. When the number of triplets increases the rate achieved is higher even though interference is present. However, it is interesting to note that for $N_t = 2$ the BER is twice (approximately) of that achieved with a single triplet. So, for example at 170cm the BER obtained with $N_t = 2$ is $1.1 \cdot 10^{-6}$ while with $N_t = 1$ is $5.7 \cdot 10^{-7}$.

Optics EXPRESS

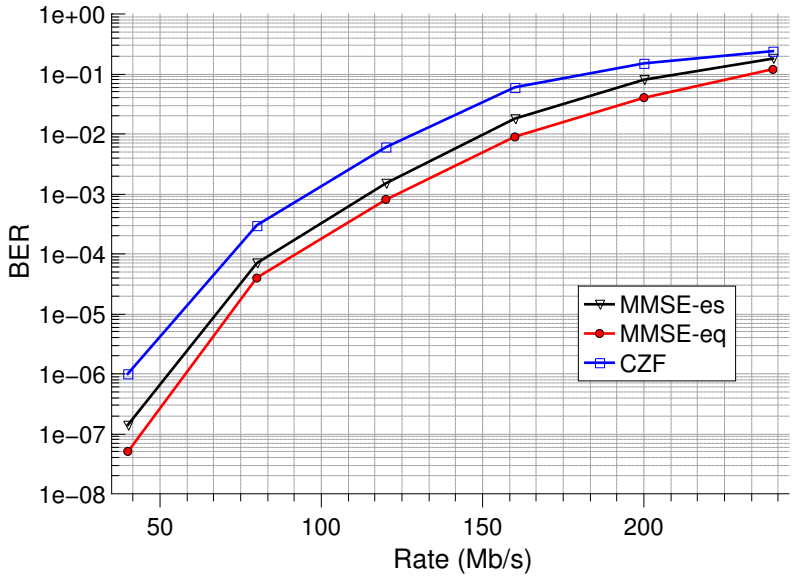

Fig. 5. BER as a function of transmission rate when the different signalling time T_p is considered.

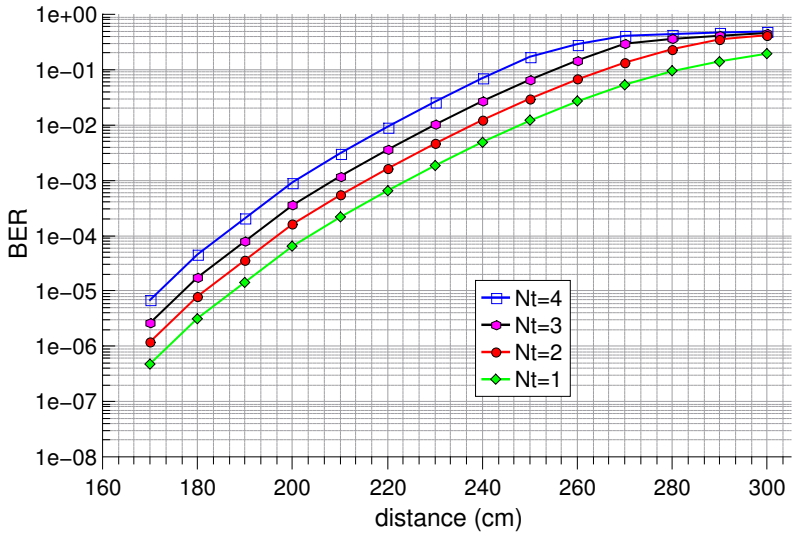

Fig. 6. BER as a function of transmission distance when different number of triplets is used.

5. Arduino implementation

Moving on the description of the implementation, we used an Arduino-Due board that presents a clock at 84Mhz. It is important to note that we aim at having the symbol rate on each branch of the order of the one [20] we generate a stream at 84Mb/s that is identically divided in 6 sub-streams ($N_t = 2$) so we have on each branch a rate of 14Mb/s.

Optics EXPRESS

This is possible by properly check the clock of the board and sending breaking messages to generate pulses that are in line, from the symbol time point of view, with the clock. Since we use the same LEDs for all reds, greens and blues, we distinguish the red of the first triplet by the red of the second one by using OAF also at the transmitter side. In this regard, Fig. 7 shows in the upper part the effect of generating different colors by using filters.

Fig. 7. Picture of the implementation of two triplets and effects of filtering with OAFs tuned on red, green and blue respectively of the first triplet.

In Fig. 7 we report also the effect of using OAFs at the receiver without taking the picture with the lens for sake of clarity of the image. Hence, the second picture of Fig. 7 reports how the photodiode tuned on the red of first triplet *sees* the six LEDs. Analogously the third picture of Fig. 7 reports the effect of filtering the six light sources with a first triplet green OAF. The fourth picture of Fig. 7 reports the effect of the first triplet blue OAF. It is interesting to note that the red OAF almost totally reduces the effect of blue LEDs and considerably attenuates the effect of green. The green OAF does not neglect the effect of red and blue due to its bandwidth. However it is able to reduce in magnitude their effect. Moreover, the blue OAF is able to suppress the red component and reduce the green one. We can affirm that, if we look at the sub-matrix modeling the channel from the two transmitting triplets to the first triplet of photodiodes, it presents very low coefficients for green and blue detected by red, sufficiently small components for red and blue detected by green and zero coefficients for reds toward blue.

In Fig. 8 we report the comparison between the simulations and the implemented case. It is worth noting that the case $N_t = 1$ differs from $N_t = 2$ since the former works with a transmission rate of 42 Mb/s while the latter transmits with a transmission rate of 84 Mb/s. In line with the results obtained in Fig. 6 we note that transmitting at a lower speed allows to preserve reliability since a lower BER is achieved and this is true at any distance between transmitter and receiver. On the other hand, the distance between the curves is very small and this allows to conclude that the model used for simulation is highly close to the reality.

Last, but not least, since we discuss earlier about color rendering features of the scheme, we do not analyze it from a quantitative point of view. Hence, in order to check how much the light obtained is likelihood to the target light, we resort to the evaluation of the color rendering

Optics EXPRESS

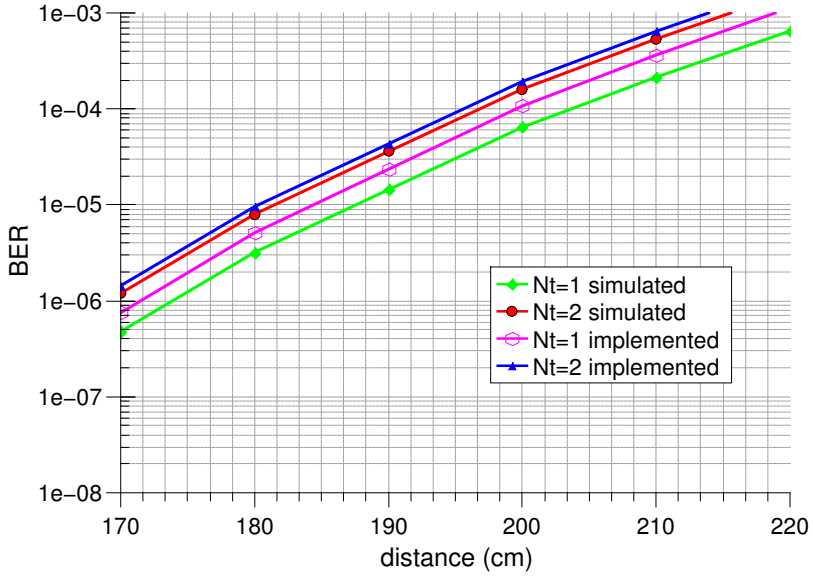

Fig. 8. BER as a function of transmission distance when different number of triplets is used. Comparison between computer simulation and implementation is reported.

index [23] that, starting from the reference illuminant D_{65} defined by CIE 1931, and by taking into account the emission of the LEDs, we achieve a value of 86. We recall that the value goes from 0 to 100 where 100 means perfect color match and very high precision white light LEDs (used only for illumination) can achieve a value of 95.

6. Conclusion

In this work we proposed MIMO-OOK scheme using multiple triplets characterized by different RGB emissions. The spectral efficiency of the system is $3N_t$ times the one achieved by single LED OOK. The scheme utilizes a preliminary optical analog filtering in order to reduce the effect of color interference and a subsequent processing is able to reduce the interference of a color on the same color, i.e. red of one triplet on the red-tuned photodiode of a different triplet. This allows also to separate channels and obtaining uncorrelated channels from the spatial diversity perspective so allowing the use of the proposed color/spatial equalization methods. Moreover, using different RGB triplets and achieving also good white illumination levels as measured by CRI. We compared the proposed scheme with the literature when white LEDs are used and we achieve the same BER with higher rate and also the implementation supports the effectiveness of the proposed system.

151.100.135.45 {ts '2018-09-20 08:09:01'}